THE EUROPEAN
PHYSICAL JOURNAL PLUS

Gold leaf tesserae: tracing the origins of gold using synchrotron-based techniques

Maria F. Guerra[1,a] ![ORCID], **Elisabetta Neri**[2,b] ![ORCID], **Martin Radtke**[3,c] ![ORCID]

[1] UMR 8233, MONARIS, CNRS-Sorbonne Université, 4 Place Jussieu, 75252 Paris, France
[2] Art, Archéologie et Patrimoine (UR AAP), Université de Liège, 10 Allée du Six-Août, 4000 Liège, Belgium
[3] Bundesanstalt für Materialforschung-und prüfung (BAM), Richard-Willstätter Str 11, 12489 Berlin, Germany

Abstract To gain insight into the possible origin of the gold used in the production of tesserae containing gold leaf less than 0.5 μm thick placed between two layers of glass, we propose a non-destructive synchrotron radiation (SR) XRF protocol based on sequential analysis under optimised analytical conditions. Using this protocol, trace element analysis is achieved with detection limits of 1–6 mg/kg. As Pt and Au have adjacent fluorescence energies, we tested the most challenging situation, when Pt is present in very low concentrations in gold. Data obtained by double-dispersive XRF (D^2XRF) and μXRF for fourth–ninth-century mosaics decorating nine Eastern and Western religious buildings show that the Eastern and Western tesserae are made from different alloys. However, these alloys are identical to those used to make gold leaf for gilding, because plastic deformation requires the use of gold alloys with high ductility and malleability. Although trace element composition of gold used in the concerned period is only available for coins, by comparing the amounts of Pt contained in the tesserae and in the coins we show that Roman tesserae are made from Roman gold, as described in the documentary sources. We observe for the Byzantine period the use of a Byzantine gold and of gold supposedly from different stages of recycling, and we suggest the use of Umayyad and Abbasid gold for the production of Islamic tesserae.

1 Introduction

The earliest known examples of precious metal-leaf tesserae date from the first century BC for gold and the second century BC for silver [1, 2]. However, the art of making mosaics containing these tesserae did not fully flourish until the Byzantine and Islamic periods, when those decorating walls and vaults achieved dazzling visual splendour, already praised in the sixth century [3]. Gold and silver tesserae were skilfully placed in mosaics to highlight the other colours or enhance them against gold backgrounds [4]. They were also placed at slightly different angles [5, 6] to optimise the effect produced by the high reflectance of the precious metals [7, 8]. The optimised orientation of the highly reflective smooth surfaces of the gold leaf tesserae relative to the position of the sources of light used in religious buildings [9–11] was used to modulate the appearance of the mosaics [12]. Under natural light (direct or diffuse), the appearance of those mosaics varies during the day with the variation of the sunlight (angle of incidence and intensity). The effect can be enhanced by combining sunlight with artificial sources of light, which can easily be moved from one precise position to another inside a building to modulate the glossy and shading appearance [13–15] of the golden parts. The effect of splendour obtained by covering entire walls and vaults with gold background mosaics needs the use of smaller quantities of gold than those perceived [1]. Gold leaf tesserae consist of a gold leaf less than 0.5 μm thick placed between two layers of glass [16, 17]. The bottom layer serves as support, and the thin top layer covers the gold leaf [18, 19]. If to let the gold shine the top layer is usually transparent to light and colourless (or in shades of natural colours [20]), when a coloured support is used, no influence on the colour of the gold leaf should be perceived. The appearance of a gilded object was shown not to be influenced by the colour of the substrate [21].

The vast majority of the publications focussing on mosaics containing precious metal-leaf tesserae focus on the analysis of the glass [19, 22–28]. Hagia Sophia [29], whose mosaics had been restored [30], is a good example of this. Reflectance spectrophotometry and colorimetry were carried out to chronologically separate the mosaics [31], optical microscopy to assess the preservation state of the tesserae [32], and the combination of SEM–EDS (scanning electron microscopy–energy-dispersive spectroscopy), XRF, and PGAA (Prompt Gamma Activation Analysis) to analyse the glass tesserae [33]. It is only recently that gold leaf tesserae from this

[a] e-mail: maria.guerra@cnrs.fr (corresponding author)

[b] e-mail: eneri@uliege.be

[c] e-mail: martin.radtke@bam.de

building have been analysed by LA–ICP–MS (Laser Ablation Inductively Coupled Plasma Mass Spectrometry) for the composition of both the glass and the gold [34].

The analysis of the metal is occasionally included in studies either to address analytical problems [35] or to provide brief additional information like the presence of Ag in the gold alloys [36–39]. For example, gold leaf tesserae from religious buildings in Rome contain in general less than 1 wt% Ag and in a few cases 7–10 wt% Ag [17, 40, 41]. Only two samples from Aquilea [16] and one from Rome [41] contain detectable amounts of Cu (0.5–1 wt%). The average composition recently obtained for 132 gold leaf tesserae from the Abbey of Stavelot in Belgium (98.3 wt% Au, 1.2 wt% Ag, and 0.5 wt% Cu) provided similar results [42]. The scarce analytical data available have been obtained mainly by SEM–EDS–occasionally by EPMA (Electron Probe Micro Analysis)—a technique with high spatial resolution but low sensitivity for the analysis of gold alloys. The quantitative results obtained may contain quite high errors, which may exceed 50% for the Ag and Cu contents in the gold alloy [43].

PIXE (Particle-Induced X-Ray Emission) being also a non-destructive technique offering for gold alloys a better compromise between spatial resolution and detection limits than SEM–EDS [44, 45], it was used by Neri et al. [46] to analyse Levantine fourth–twelfth-century gold leaf tesserae. The data showed that Cu is present in amounts < 1 wt%, with the exception of one tesserae (from the Church of the Nativity in Bethlehem [47]). Data published for Qusayr Amra (Jordan) [48] and the Umayyad Mosque of Cordoba in Spain [49], obtained by PIXE, do not include the amounts of Cu. In the tesserae from Cordoba ([49] Fig. 2D) the Cu seems to range from *c.* 0.5 wt% to the detection limits (160–500 mg/kg [50]), and in the one from Qusayr Amra, it should be under the detection limits (< 90 mg/kg [44]).

PIXE did not provide the trace element composition of the gold leaf tesserae. Only a highly sensitive technique with high spatial resolution allows trace element analysis of such small and thin layers of gold. To our knowledge, only two publications focus on the origin of the gold. By combining EPMA with LA–ICP–MS, Panhuysen et al. [51] analysed gold leaf tesserae from the basilica of St. Servatius in Maastricht and from the Charlemagne's Palatial Chapel of Aachen. A previous publication only indicates that those from Aachen split into three compositional groups [52]. The second publication is an extensive study by LA–ICP–MS by Schibille [34], who provides major and trace (Pt and Pd) element analysis for gold leaf tesserae from Hagia Sophia, the Mosque of Damascus, the residential site at Khirbat al-Minya, the Church of St. Mary at Ephesus, and the Roman villa of Noheda.

Although LA–ICP–MS has the analytical characteristics needed for the analysis of gold leaf tesserae, sampling with laser spot diameters of several tens of μm (typically 80 μm, but in particular cases reduced to 40 μm [53, 54]) produces craters in the gold leaf. To improve accuracy, several areas are sampled, which partially destroys the sample. In addition, the ablated volume contains the gold leaf and the first layer of glass, making it more difficult to calculate the concentrations of the trace elements contained in the gold alloy [53]. To overcome these problems, we propose in this work a non-destructive protocol based on XRF methods, which allows not only repeated analysis of the same areas of the gold leaf by using either the same technique or other techniques, but also preservation of the samples for any further analytical study. This effective and innovative protocol offers major and trace elemental analysis by using synchrotron-based (SR) XRF techniques. which have been optimised for the analysis of gold alloys at BESSY II.

One of the most important elements in gold fingerprinting is Pt, as discussed in previous work [45, 55–57], whose amounts are sometimes combined with the trace amounts of Pd present in the gold [58–60]. However, whilst for Roman and Islamic gold several trace elements have been measured [61–64], Pt is the only trace element so far analysed for Byzantine gold [65]. Present at very low concentrations in gold, this element is specially challenging to analyse by SRXRF methods. We have discussed these analytical difficulties in previous publications [66–68]. The major difficulty comes from the fact that the characteristic X-ray lines of Pt overlap those of the major element, Au. To solve the severe peak overlap problem when using an energy-dispersive setup, we propose in this work to use a double-dispersive XRF system (D^2XRF). We test the applicability of this technique to the study of gold leaf by analysis of a set of tesserae from fourth–ninth-century mosaics, collected in nine Eastern and Western sites. These mosaics cover a long period, when changes in the gold supply should be observed, when Byzantine gold is used and therefore, when Pt is commonly used to search for the origin of the gold.

By comparing the composition of the gold leaf with the published composition of gold objects from the same periods (Roman, Byzantine, and Islamic) we provide below an in-depth discussion on the possible origin of the gold. As both the making of gold leaf and the gilding processes described in documentary sources appear sometimes related to gold coins, we also offer a discussion on this possibility below.

2 Materials and methods

XRF methods are used in this study to determine the composition of the gold alloys. XRF is a powerful analytical technique that can be used to determine the elemental composition of a material. This technique is non-destructive and can be used to analyse trace elements in gold alloys by measuring the intensity of the emitted characteristic X-rays. These elements can be identified by comparing the measured characteristic X-ray energies with those of known standards. The concentration of each element can be quantified by calibration against standards of known composition or by using well-established calculations. However, this technique is strongly matrix-dependent, and therefore, not all elements can be measured simultaneously with high sensitivity.

In order to propose an effective protocol offering major and trace elemental analysis of the gold leaves contained in tesserae, based on the non-destructiveness of XRF methods, we test the possibilities of the sequential analysis of the same areas at different

analytical conditions. This protocol, assessed on three gold standards containing different amounts of trace elements, is discussed in light of its advantages and disadvantages over LA–ICP–MS. As Pt is the only know trace element of Byzantine gold, we concentrate here on the measurement of this element using the D^2XRF configuration described below, developed to optimise the detection limit of this trace element. Because of the limited synchrotron beamtime, the major elements of the gold alloys (Au, Ag, and Cu) were obtained by μXRF with a M4 Tornado from Bruker, which comprises a Rh X-ray source (50 kV, 300 μA) coupled to a SDD detector and a poly-capillary lens offering a spot size down to 25 μm. Spectra deconvolution was made using the Bruker M-Quant software, and the accuracy of the quantitative results was validated by the analysis of a set of gold standards [69].

2.1 SRXRF protocol and advantages over LA–ICP–MS

LA–ICP–MS is a powerful tool for rapid trace and ultra-trace multi-element analysis of solid samples, and it also provides isotopic analysis. The sample is ablated by a focussed laser beam and is then transported by a carrier gas (Ar or He) into an inductively coupled plasma ion source. In the plasma, which is around 8000 °C hot, the tiny sample particles are atomised and positively ionised, accelerated, and transported into the high vacuum of a mass spectrometer. There, they are separated according to their mass-to-charge ratio and energy-to-charge ratio and detected in a time-resolved manner.

LA–ICP–MS is a widespread technique frequently used to analyse ancient goldwork, because as coupled with laser ablation it allows, without preparation of the surface, spatially resolved elemental analysis with short acquisition times and good detection limits. The ablated crater is under 100 μm diameter and the volume ablated by single-spot analysis is quite small, although to improve accuracy repeated analysis is carried out for example in line scan mode. Like synchrotron-based methods, and although mobile equipment has been developed for in situ analysis [70], LA–ICP–MS requires moving the object to the laboratory. Perhaps the main advantages of LA–ICP–MS over SRXRF methods are the use of pre-ablation to avoid possible surface heterogeneity and the fact that the depth of the analysis only depends on the depth of the ablation. For SRXRF methods this parameter is influenced by the matrix, mainly due to self-absorption. The depth of the analysis depends on the detected fluorescence energy and thus differs for each configuration and detected element. It can be estimated from Lambert–Beer's law and the measurement geometry [71]. For an exit angle Θ density ρ cross section μ and assuming that about 95% of the fluorescence radiation comes from within the depth $D_{Information}$ it can be estimated as:

$$D_{Information} = \frac{0.05}{\mu * \rho * \sin\Theta}$$

For gold alloys, the information depth is typically about 5 μm for Cu and 20 μm for Ag, but because in the present case the gold leaf is typically less than 0.5 μm thick, the whole volume is analysed.

Contrary to LA–ICP–MS, SRXRF methods are fully non-destructive. This is obviously of great value for the analysis of ancient objects. Although the craters produced by LA are small, the analytical results obtained by LA–ICP–MS can obviously not be verified. By using SRXRF methods, it is possible to repeat the analysis of the same area either by using the same method or by using other methods. In addition, SRXRF methods offer high-resolution in-air analysis for objects of unlimited size, contrary to an ablation cell when using LA–ICP–MS [72]. SRXRF also offers scanning mode with a μbeam. In the case of composite objects, such as complex gold jewellery made by joining many different small parts, this allows to analyse all parts and the joins non-destructively. This can be carried out either by using a single-spot mode or a scanning mode.

Therefore, it is mainly the question of the achievable detection limits and accuracy of the measurements that needs discussion in the case of gold leaf. LA–ICP–MS detection limits are lower than 1 mg/kg for all elements in all performed analyses of different gold calibration materials. If the deviations from the certified values depend on the applied calibration technique, they are typically in the range of 10–15%. Pt can be reliably measured in a sample containing as low as 5 mg/kg [73] or less [54]. XRF has in general poorer detection limits, which can, however, be highly optimised by combining measurements based on different excitation energies and detection methods.

To lower the detection limits and improve accuracy and precision [74] when analysing by SRXRF gold leaf tesserae, each sample can be analysed under three analytical conditions: (1) with 10 keV excitation energy and an SDD detector to measure elements up to Zn (the Au M-lines serve as internal standard); (2) with 35 keV excitation energy and a Si(Li) detector with a 400-μm-thick Al filter to suppress the predominant Au L-lines (pile-up peak and detector saturation are avoided) to measure the characteristic lines of the heavier elements which are above 15 keV (the Au L-lines serve as an internal standard); (3) elements with characteristic lines that overlap the Au lines (e.g. As, Bi, Pb, Pt) are measured by the above-described D^2XRF.

Using this protocol at the Helmholtz-Zentrum in Berlin, we determined the detection limits for the elements contained in three gold standards (NA30 and NA31 from Aurubis AG and RM 8058 from the Royal Canadian Mint). The limits of detection attained, summarised in Table 1, are 1 mg/kg for Zn to 4 mg/kg for Cr for the first group of elements, c. 6 mg/kg for the second group, and typically 4 mg/kg for the third group. The uncertainty of the measurements, mainly caused by measurement statistics, is typically under 5% relative.

On the basis of these results, we can affirm that major and trace element analysis can be performed by sequential analysis with synchrotron-based techniques only. Although slightly poorer than the detection limits of LA–ICP–MS, the detection limits obtained using this SRXRF protocol range from 1 to 6 mg/kg that we can assume sufficient for fingerprinting gold leaf tesserae. As the

Table 1 Limits of detection determined for standards NA30 and NA31 from Aurubis AG and RM 8058 from the Royal Canadian Mint using IUPAC definition

EDXRF	Cr [mg/kg]	Mn [mg/kg]	Fe [mg/kg]	Co [mg/kg]	Ni [mg/kg]	Cu [mg/kg]	Zn [mg/kg]
Excitation [keV]	10	10	10	10	10	10	10
NA-Au-30	9	7	34	10	48	99	11
LOD	4	4	2	2	2	2	1

EDXRF	Pd [mg/kg]	Ag [mg/kg]	Cd [mg/kg]	Sn [mg/kg]	Sb [mg/kg]	Te [mg/kg]
Excitation [keV]	35	35	35	35	35	35
NA-Au-30	55	10,000	10	50	9	10
LOD	6	9	10	4	2	2

D^2XRF	Pb [mg/kg]	Bi [mg/kg]	D^2XRF	Pt [mg/kg]
Excitation [keV]	16.5	16.5	Excitation [keV]	11.7
NA-Au-31	90	100	RM8058	40.8
LOD	4	9	LOD	1

The determination of the Pt limits (D^2XRF) is described in Radtke et al. [76]. The fine-tuning of the excitation energy can be used to lower the detection limit for an element of interest

detection of Pt is the most challenging situation in the case of gold alloys [75, 76], and because Pt is one of the most characteristic elements of gold and the only available for Byzantine gold, we analysed in this work the gold leaf tesserae at optimised conditions by D^2XRF. This technique is shortly described in the next section.

2.2 Double-dispersive XRF (D^2XRF)

For the analysis of the gold leaf tesserae, we used an X-ray fluorescence setup that combines a flat crystal geometry with an energy-dispersive pnCCD detector. This configuration allows improving the detection limits of the trace elements contained in a gold-based matrix when the characteristic elements to be detected have adjacent fluorescence energies. This setup, called D^2XRF, which is based on the combination of a crystal analyser with an energy-resolving single-photon counting pnCCD, enables the simultaneous analysis of trace and major elements. The choice of a flat crystal geometry was motivated by the desire to achieve the simplest possible setup. The reflectivity and d-spacing of the crystal are chosen to optimise the count rate and the energy resolution, respectively. The energy-dispersive pnCCD detector was chosen for its ability to suppress scattered radiation and to provide high-energy resolution. The results of the first experiments and the technical details were presented in Radtke et al. [76].

Figure 1 shows a schematic view of the setup. This setup allows simultaneous wavelength-dispersive measurements for an energy range of around 1 keV. To achieve reliable data, a strictly followed measurement sequence was developed. It consists of the exact positioning of the sample, thus assuring the accurate energy calibration of the setup by controlling the position of the Au L-line before the subsequent measurement of the fluorescence lines with an excitation energy of 17 keV. The exact positioning of the sample is essential to ensure the correct attribution of the measured lines, which is complicated by the number of lines and the minor energy differences involved. The Au L-line also serves as internal standard to improve the precision of the quantitative analysis. The typical acquisition time for the D^2XRF measurements is 1000 s with a beam size of $500 \times 500\ \mu m^2$.

In the case of the gold leaf tesserae, the measurements were taken at the mySpot beamline [77], one of the two high-energy beamlines for XRF measurements at the synchrotron BESSY II. The energy of the X-ray beam was tuned by a double-crystal Si(111) monochromator (DCM) and a mirror to suppress higher harmonics.

2.3 Analysed tesserae and sample preparation

The gold leaf tesserae analysed in this study were collected in situ (by E. Neri) from mosaics dating from the fourth to the ninth century during archaeological excavations or restorations of religious buildings in nine sites. Hierapolis and Mar Gabriel in Turkey and Jerusalem in Israel are Byzantine sites. Arles in France and Milan in Italy are Late Roman sites, whilst Rodez and Nevers in France and Aachen in Germany are situated in Romano-Barbarian kingdoms.

Gold leaf tesserae from mosaics in some of those sites have already been published [46, 78, 79]. In this work we analyse additional tesserae from the Eleona basilica on the Mount of Olives in Jerusalem (fourth century), the church of St. Philip in Hierapolis (from both the sixth-century phase and a ninth-century restoration), the cathedral of St. Cesaire in Arles (late fourth to early sixth century), the baptistery of the Cathedral of St. Cyr and St. Juliette (sixth century) in Nevers, and the church of San Lorenzo in Milan (late fourth to early fifth century). We also considered tesserae collected in the church of St. Peter in Rodez and in the Monastery of Mar Gabriel (sixth century) as well as from the Palatine Chapel in Aachen. The latter come from the original decoration of the imperial building founded by Charlemagne in 792 [80]. Finally, we included tesserae from the Mosque of Damascus, in Syria, that was founded by the Umayyad caliph Al-Walīd.
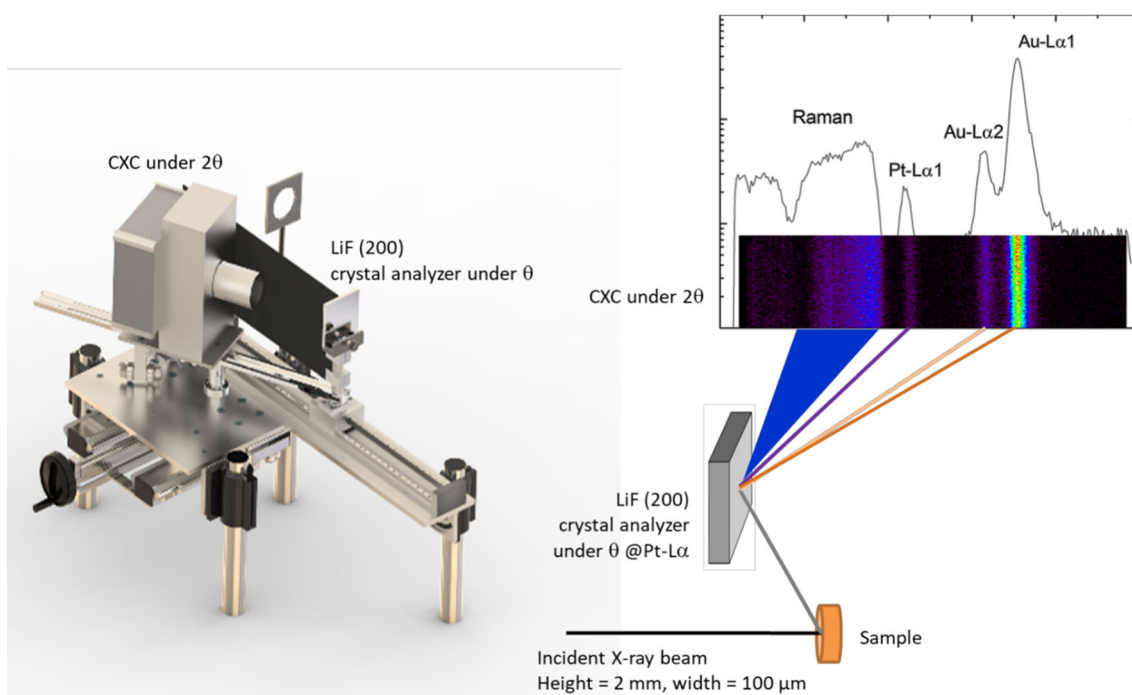
Fig. 1 Schema of the principle of the D^{2}XRF. The exciting monochromatic beam of 11.564 keV produces Pt-Lα fluorescence in the sample. The characteristic radiation is dispersed to the detector by a LiF (200) crystal. The energy resolution of the detector enables to efficiently suppress the background and separate the fluorescence line from the Raman scattering

Fig. 2 One of the analysed tesserae (0.8 cm height, 0.9 cm width, 1.35 cm length) after removing of the top glass layer for analysis, with a detail of the gold leaf under the SEM (images M. F. Guerra)
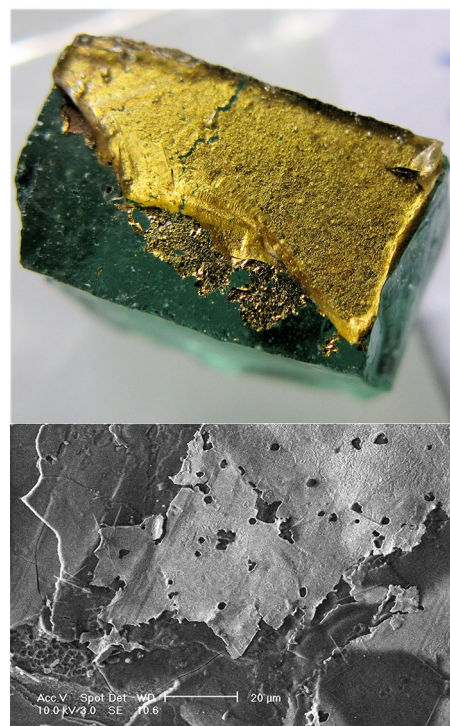
For each tesserae, the μXRF and D^{2}XRF analyses were carried out directly on the gold leaf made apparent by the removal of 1–2 mm^2 of the upper glass layer, as shown in Fig. 2.

3 Results and discussion

3.1 The gold alloys

Table 2 summarises the data obtained in this work by µXRF for the major elements of the gold alloys used in the production of the analysed gold leaf tesserae. Data previously obtained for the same sites [46, 78, 79] have been included in the discussion offered below as well as additional data summarised in Table 3, obtained by PIXE (at the same conditions as used in previous work [46]) for Aachen, Arles, and Milan.

We plotted in Fig. 3 all the gold leaf analysed in this work with data published for Rome and Aquilea (second–fourth century) and other Italian sites (fifth–sixth century) [41]. We added data published by Neri et al. [46] for the baptistery of the Basilica of Gortyna (seventh century), the Triconch church of Mount Nebo (fifth–eighth century), Qusayr Amra (eighth century), and the Church of the Nativity in Bethlehem (twelfth century). Finally, we added tesserae from Aachen and Maastricht published by Panhuysen et al. [51] (from Fig. 19), from the Mosque of Cordoba published by Gómez-Morón et al. [49] (from Fig. 2D) and from Hagia Sophia, the Mosque of Damascus, Khirbat al-Minya, and Noheda published by Schibille [34] (from Fig. 29B). We observe that, as expected, the majority of the analysed gold leaves are contained in an area characterised by less than 4 wt% Ag and 1 wt% Cu, corresponding to gold alloys containing more than *c.* 95 wt% Au. These high-purity gold alloys are used regularly for gilding, a plastic deformation process requiring the use of alloys with high ductility and malleability.

We plotted in the same figure the tesserae produced until the sixth century (Rome, Aquileia, Noheda, Jerusalem, and Milan) separated from those made between the sixth and the eighth century. The later were plotted by origin. Although some alloys used in the Eastern sites are observed in Western sites, all tesserae containing higher amounts of Cu and Ag come from Eastern sites; the large majority being those from al-Minya and Damascus. A large part of the tesserae collected at Aachen, Maastricht, and Arles contain very low amounts of Cu and Ag and, therefore, appear grouped together on the top of the ternary diagram. These results tend to confirm Ristow's [81] suggestion on a possible local production. Indeed, the excavations carried out at Aachen delivered materials related to a workshop producing tesserae from the Carolingian period until the tenth century [80].

Nevertheless, these very high-quality alloys are not particular to the mentioned three sites, because the same alloys were observed for other sites included in the diagram. As mentioned, high-purity gold alloys are used regularly for gilding. Today in Paris, Dauvet uses a 23.5-carat gold alloy (98 wt% Au, 1 wt% Ag, and 1 wt% Cu) to produce gold leaf [82].

3.2 Gold leaf tesserae and gilding

Gilding was used very early in the production of a large sort of objects. The process of hand-making gold leaf is the work of a specialised artisan, the goldbeater, attested not only in Egypt ("chief of the makers of thin gold" [83] and "chief of the makers of gold leaf" [84], among others [85]), but also under the Romans (chapter 28 on gold and silver in the Edict on Maximum Prices (AD 301) by Emperor Diocletian [86, 87]). They formed a guild with gilders [88, 89]. Indeed, goldbeaters need to have great knowledge of the practice of beating gold into leaf, but need no knowledge of the practice of goldsmiths' techniques (embossing, soldering, engraving, chasing, etc.).

Hand hammering gold into leaf is a long process. According to Berthelot and Ruelle [90], in one day a goldbeater can produce 150 gold leaves from a solid gold ingot. Although difficult to calculate due to the imprecision of the ancient treatises, we estimated the gold leaf according to Pliny (book 33, chapter 19.62 [91]) to *c.* 7.4 cm in side length and *c.* 0.34 µm in thickness, based on Roman units and 750 produced leaves. We also estimated the gold leaf according to Cennini (chapter 139 [92]) and Vasari (chapter 28 [93]) using the length of the *braccio fiorentino* [94] and the weight and fineness of the gold coins mentioned in the recipes (the *ducat* during Cennini's lifetime [95, 96] and the Florence *scudo* during Vasari's lifetime [97]). For the side length given by Pliny, Cennini's recipe indicates gold leaf *c.* 0.33 µm thick (for 100 leaves, but 0.23 µm for 145 leaves). Gold leaf based on Vasari's recipe is *c.* 0.2 µm in thickness and *c.* 7.3 cm in side length. The gold leaf offered today by goldbeaters is similar, c. 8 cm in side length and 0.17–0.2 µm in thickness [18, 82].

Gold alloys with the adequate physical properties for plastic deformation, high malleability and ductility [98, 99], are necessary to produce gold leaf. Diderot and D'Alembert indicate the use of 23 ¾ carat gold. Similar qualities are both mentioned in commission contracts passed with goldbeaters in the seventeenth and eighteenth centuries [100] and produced today [82]. We plotted in Fig. 4 the gold leaf tesserae with gilded objects (gold leaf < 1 µm) and gold leaf (> 1 µm) and foil (< *c.* 30 µm) of very different chronology, although produced around the Mediterranean basin. They are Egyptian, Middle Kingdom to Roman Period [75, 101–103]; Hellenistic and Roman, from Greece [104], Italy [105], and Thracia [106]; and mediaeval [21, 107, 108]. The gold leaf < 1 µm thick (tesserae and gilding) forms the same chemical pattern in the ternary diagram, and the majority contain more than 97 wt% Au. These are the most appropriate alloys to be worked by plastic deformation.

The treatises by Cennini and Vasari mentioning coins in the recipes for making gold leaf, and fifteenth-century commissioning contracts for paintings and altarpieces [109] mentioning the "good fine gold" of the *ducats* [110], we considered in Fig. 4 the alloys used to mint late Roman (third–fifth century [111–117]), Byzantine (fifth–ninth century [65, 118]), and Islamic (eighth–eleventh century [63, 64]) coins. The chemical patterns are identical, because with the exception of periods of gold scarcity [119], gold coins

Table 2 Composition of the gold leaf tesserae obtained by μXRF and D^2XRF (nd = not determined)

Site (country)	Reference	μXRF (wt%)			D^2XRF (ppm)
		Au	Ag	Cu	Pt
Damascus (Syria)	DA2	96.1	3.1	0.8	231
	DA3	96.5	2.6	0.9	231
	D16	95.0	4.0	0.9	218
Mar Gabriel (Turkey)	MG10a	96.3	3.5	0.3	153
	MG10b	94.2	5.1	0.7	153
	MG11	98.6	1.3	0.1	180
	MGa	93.2	5.5	1.3	<1
	MGb	95.5	3.4	1.1	nd
	MGc	95.9	3.3	0.8	nd
	MGd	96.7	2.3	1.0	220
	MGe	95.8	2.6	1.6	442
Hierapolis (Turkey)	HA1	95.0	4.8	0.2	198
	HA7	98.3	1.5	0.3	134
	HA9	96.7	2.9	0.4	427
	HA12	97.3	2.0	0.6	170
	HA14	99.3	0.3	0.4	230
	HA20G	95.6	3.5	0.8	185
	HA20P	96.5	3.1	0.4	185
Jerusalem (Israel)	MT0	98.5	1.4	0.2	229
	MT2	97.0	2.6	0.4	155
	MT3	97.3	2.3	0.4	104
	MT5	98.5	1.3	0.3	nd
	MT4	97.1	2.4	0.5	293
	MT1	97.7	1.9	0.3	1552
Milan (Italy)	M6	98.0	1.7	0.3	<1
	M10	95.8	3.6	0.6	<1
	M12	97.6	2.1	0.3	nd
	SL10	98.8	1.0	0.2	283
Arles (France)	A1B	98.1	0.6	1.3	205
	A2B	99.0	0.3	0.7	212
	A3b	98.8	0.5	0.7	253
Nevers (France)	NE5	95.4	3.8	0.9	298
	NE6	94.7	3.3	2.0	<1
	NE7	94.3	3.5	2.3	nd
	NE8	95.2	3.0	1.8	<1
Rodez (France)	RZ2.1a	95.7	2.8	1.4	639
	RZ2.1b	96.6	2.9	0.4	193
	RZ3	97.5	2.1	0.4	nd
	RZ7	97.2	2.2	0.6	nd
	RZ7 B	97.6	2.2	0.2	168
	RZ10	96.8	2.7	0.4	nd
	RZ12	98.5	1.1	0.3	nd
Aachen (Germany)	ACH3B	98.8	0.6	0.6	215

Table 3 Composition of the gold leaf tesserae obtained by PIXE at the same conditions as in Neri et al. [46]

Site (country)	Reference	PIXE (wt%)		
		Au	Ag	Cu
Arles (France)	A1	99.4	0.3	0.3
	A2	98.3	1.5	0.2
	A3	99.6	0.3	0.1
	A4	99.6	0.3	0.1
Milan (Italy)	MISL3	98.6	1.3	0.2
	MIISL4	98.3	1.3	0.4
Aachen (Germany)	ACH2	96.4	3.3	0.3
	ACH3	99.5	0.4	0.1
	ACH4	99.8	0	0.2
	ACH5	100	0	0
	ACH10	99.9	0	0.2
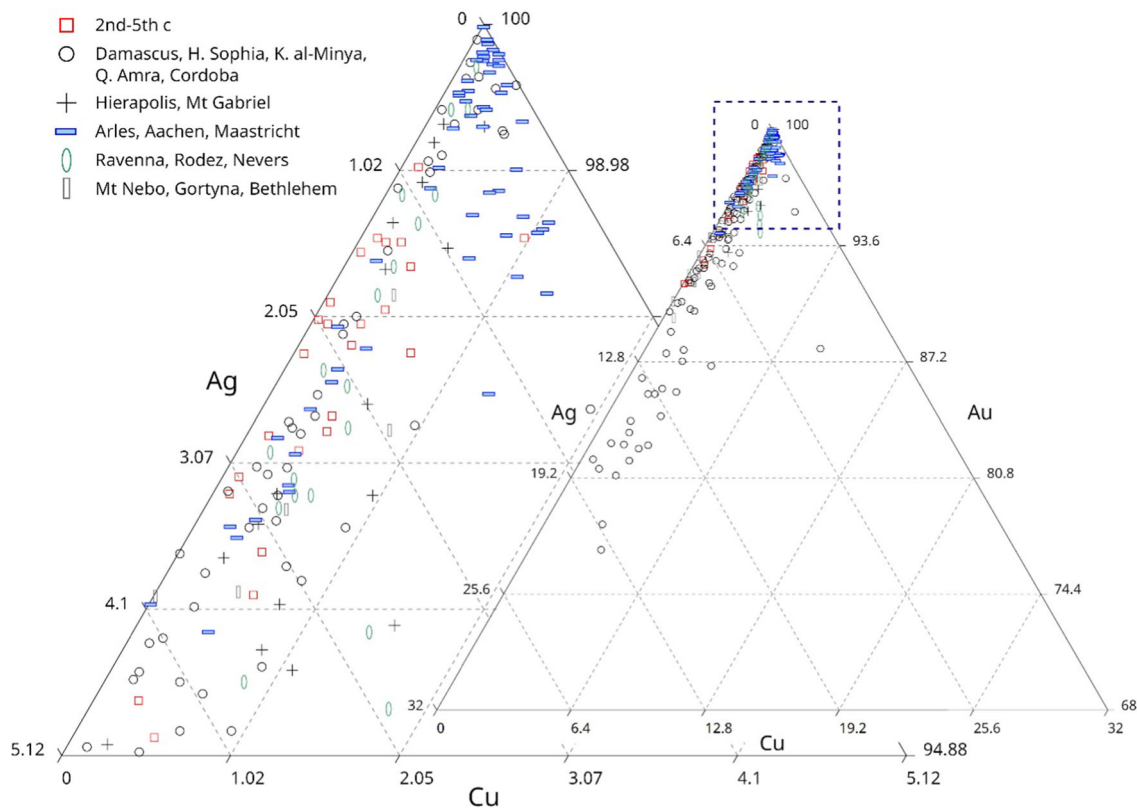
Fig. 3 Au–Ag–Cu ternary diagram showing the composition of all the gold leaf tesserae mentioned in the text, with a zoom showing those produced from the highest purity alloys

are also struck with high-purity alloys. However, although many alloys used to make gold leaf are found among the most common monetary alloys, many of them are not observed.

Even if coins may have been used in particular cases, this result does not support the hammering of gold coins into leaf to produce gold tesserae during the concerned periods. Documentary sources also do not support hammering coins into gold leaf. As the gold is provided to goldbeaters and goldsmiths by the clients [89], it is important to mention Fortunatus of Grado's will (AD 824–5) where 12 lb. of gold is said to be given for gilding, whilst the work of a goldsmith to enlarge a small censer was paid in *solidi* ([120] in Table 11.1). Making high quantities of gold leaf by hammering coins in circulation instead of ingots would involve too high costs for the treasury.

In the recipe for making gold leaf of the so-called Lucca manuscript (the Liber Pontifica or codex Lucencis 490, late eighth–early ninth century) where a whitish gold is obtained by mixing 1 oz. of "Byzantine gold" with 1 oz. of "clean silver," an ingot is hammered into gold sheets "weighing 5 Byzantine *tremis*," which are then hammered into gold leaf (recipe 246 A in [121]). The *tremis* [122,
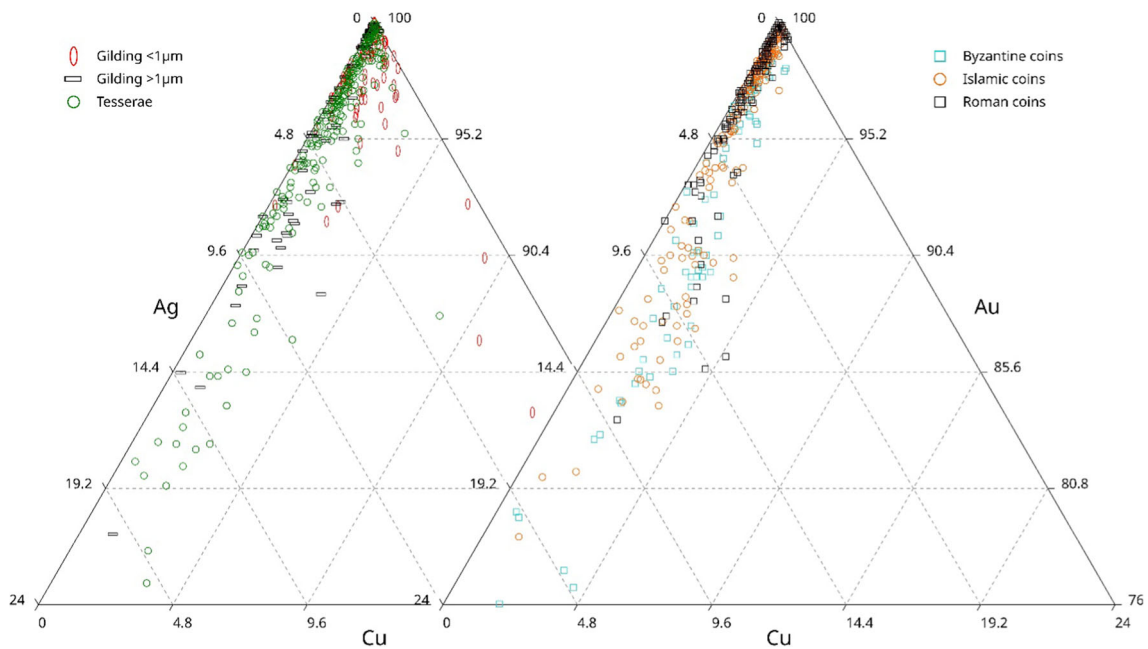
Fig. 4 Au–Ag–Cu ternary diagrams comparing on the left the composition of the gold leaf tesserae with leaf and foil mentioned in the text. On the right are plotted for comparison the composition of the alloys used to mint Roman [111–117], Byzantine [65, 118], and Islamic [63, 64] coins

123] is a coin used here to indicate the weight of the gold sheet. Coins were often mentioned as standards of purity and weight. They were simple ways of representing quantities of gold [124]. For example, in some tenth-century transactions documents, the *solidus* is cited as "*solidi*," "*solidi* of silver," and "*solidi* of gold" to express the value of the prices [125] and Al-Razi (AD 865–923) used the *dirham* and the *mithqal* to quantify metals in the Book of Secrets, because these coins were among the most standardised weights available during his lifetime [126].

3.3 Pt and the origin of the gold

The amounts of Pt obtained for the 34 tesserae selected for analysis by D^2XRF are summarised in Table 2. The majority contain Pt spanning from *c.* 100 to 300 mg/kg. Only four tesserae, all from different sites, contain higher amounts of Pt, between 400 and 1550 mg/kg. The presence of Pt in gold indicates the use (or/and reuse) of alluvial gold. Nevertheless, five other tesserae (two are from Milan and two from Rodez) contain amounts of Pt under the detection limits, indicating the probable use of gold from other sources. It is difficult to suggest its origin. Like the Byzantine fiscal system, which was based on taxation [127], the Roman treasury was a centralised office that controlled all aspects related to precious metals. The gold processed by the treasury was received from taxes and was captured as booty and obtained by gold mining [128]. Both auriferous quartz and alluvial deposits were exploited under the Romans [129–131] and the Byzantine [132–135] and the Theodosian code refers to labour associated with gold mines in Illyricum, Macedonia, Thrace, Pontus, Dacia, Moesia, Italy, Gaul, etc. [136]. Like the owners of the gold deposits, the gold washers and the gold miners paid a fixed annual tax to the treasury in "gold dust" and the rest of the gold that they recovered was forcibly sold to the treasury at a fixed price (Theodosian code 10.19 [137] and Justinian code 11.7 [138]).

Therefore, to look for the origin of the gold used in the production of the gold leaf tesserae, we compare below by period the amounts of Pt contained in the gold leaf with the amounts published for gold coins, which were minted by the treasury. Trace element composition is only available for this type of gold production.

3.3.1 Roman and Byzantine gold leaf

We compare in Fig. 5 the amounts of Pt contained in fourth–early sixth-century tesserae with those contained in Roman coins [111, 112]. We added to the diagram the data published for the Roman villa of Noheda (from [34] figs. 29A and C). We observe that with the exception of two from Milan, all tesserae contain the amounts of Pt expected for Roman gold. However, if the tesserae from Arles and from Jerusalem are close to the fourth–fifth-century Roman coins, those from Noheda correspond better to the coins minted in the third century. Although impossible to conclude on a different chronology, it is noticeable that they are contained in the same chemical group as the coins minted before AD 350, which means before the currency reforms in AD 365–368 [139].

We compare in Fig. 6 the amounts of Pt contained in the sixth-century tesserae with Byzantine coins [65], and we added the data published for Hagia Sophia (from [34] figs. 29A and C). The Byzantine gold minted in the sixth and seventh centuries contains on
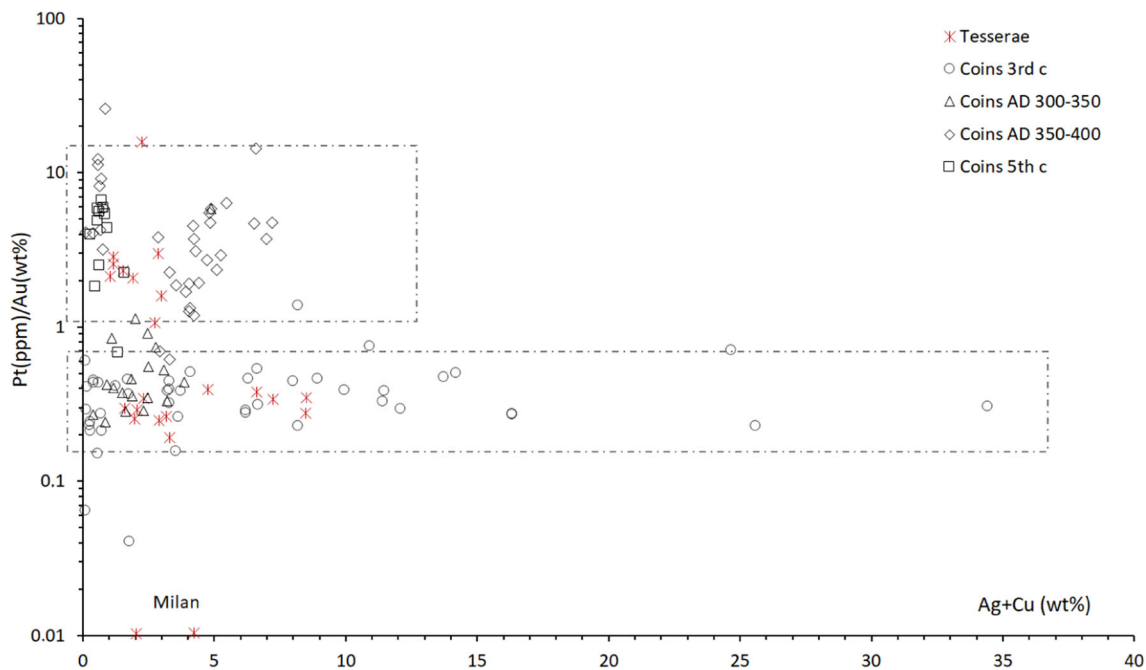
Fig. 5 Ratio Pt/Au versus the amounts Ag + Cu for fourth to sixth-century tesserae mentioned in the text compared with the data published for Roman coins [111–117] and published by Schibille [34] for gold leaf tesserae from Noheda

average the same amounts of Pt, and these amounts are the same observed for many of the tesserae. When we add to Fig. 6 one tesserae from Aachen (eighth century), one tesserae from Hierapolis (ninth century), and the Byzantine coins struck in the eighth and ninth centuries, we observe that they also contain the same amounts of Pt. This is explained by considering the Theodosian code (12.6. 12 and 13). In the case of taxes paid in money, to avoid fraud, the coins were "reduced to a firm and solid mass of pure gold," and the ingots obtained were tested and certified with official stamps [140] in a sub-department of the treasury to be used in the production of objects [141, 142]. Two found in present Romania have the official stamps of Sirmium [143]. The flow of precious metals from the provinces to the imperial centre indicates that the new issues were struck using older issues from the payment of taxes returned to the treasury [136] as well as with gold arriving in dust and bullion. Any other gold object produced by the treasury or by private gold workers (goldsmiths and goldbeaters) should have been made from the same gold.

However, some tesserae have lower amounts of Pt than those observed for the Byzantine coins. This can result from the reuse of gold tesserae or simply the use of gold alloys made by mixing gold from different origins in particular periods, for example when the Islamic empire was established in the West. One tesserae from Mar Gabriel and two of the analysed three from Nevers not containing Pt are made from another type of gold.

3.3.2 Islamic gold leaf

We compare in Fig. 7 the amounts of Pt contained in the tesserae from the Mosque of Damascus, in Umayyad and Abbasid coins [63, 64], and in Byzantine coins issued from *c*. AD 650 to 900 [65]. We also added the data published by Schibille [34] for the Mosque of Damascus and Khirbat al-Minya (from figs. 29A and C). As expected, the amount of Pt contained in the Umayyad and Byzantine gold are identical. The Islamic gold coin, the *dinar*, introduced in AD 696–7 by the reform of Abd al-Malik [144], was minted by melting down the gold in circulation [63]. The transitional Arab-Latin coins struck before the *dinar* in the mint of Carthage [145] are made from Byzantine gold containing higher amounts of silver.

After the Islamic conquest, salaries and taxes were calculated in Islamic and Byzantine gold coins (*e.g.* the Nessana papyrus [146, 147]) and gold circulated under different forms [148], in "bars of gold" and "purses of money in coins" (Book of Gifts and Rarities, eleventh century, [149]). However, and although the Umayyad rulers struck the mentioned transitional coins, the gold Umayyad hoards found in Syria and Palestine include only *dinars* [150], which supports the suggestion on the melting down of the Byzantine coins (and the transitional ones) to issue the *dinar*. Therefore, with time, the recycled Byzantine gold diluted into the new huge Islamic gold mass in circulation. From this dilution results a decrease of the amounts of Pt under the Abbasids. This can be used to explain the splitting into two groups in Fig. 7 of the Umayyad and the Abbasid coins. The tesserae are divided into the two groups suggesting the use of both a "Byzantine/Umayyad" and an "Abbasid/local" gold. Although more analytical data are necessary to provide further discussion on the origin of the gold used in the production of the Islamic gold leaf tesserae, it is noticeable that the
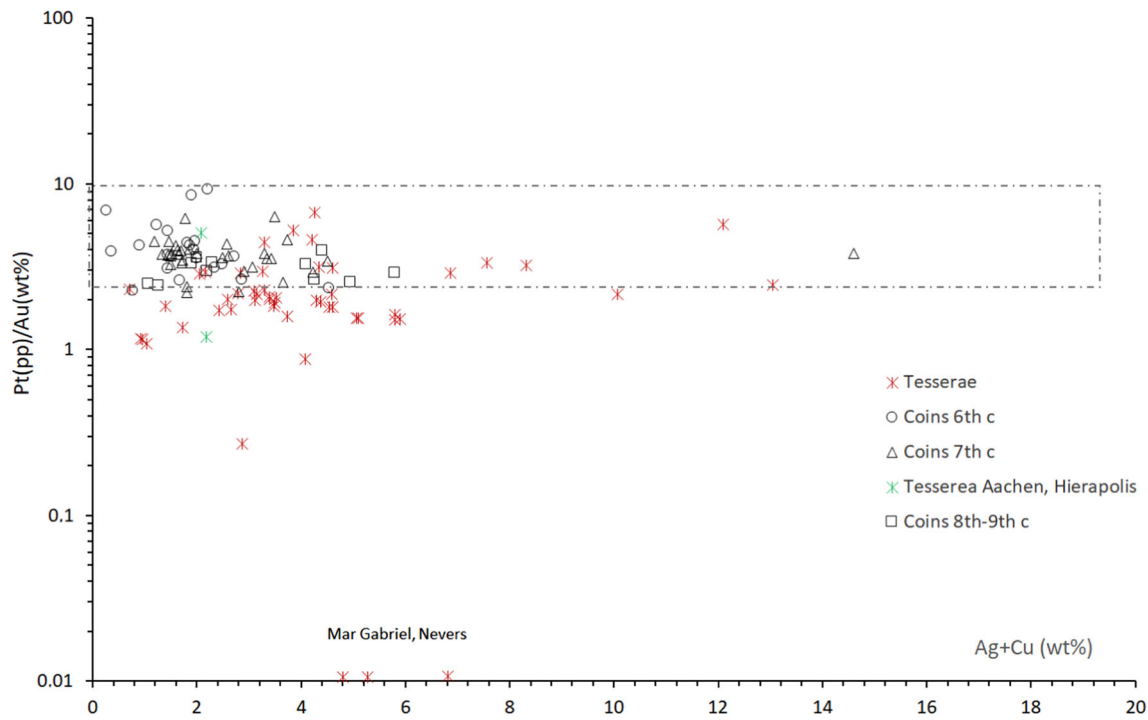
Fig. 6 Ratio Pt/Au versus Ag + Cu for sixth-century tesserae mentioned in the text compared with data published for Byzantine coins [58] and published by Schibille [34] for gold leaf tesserae from Hagia Sophia
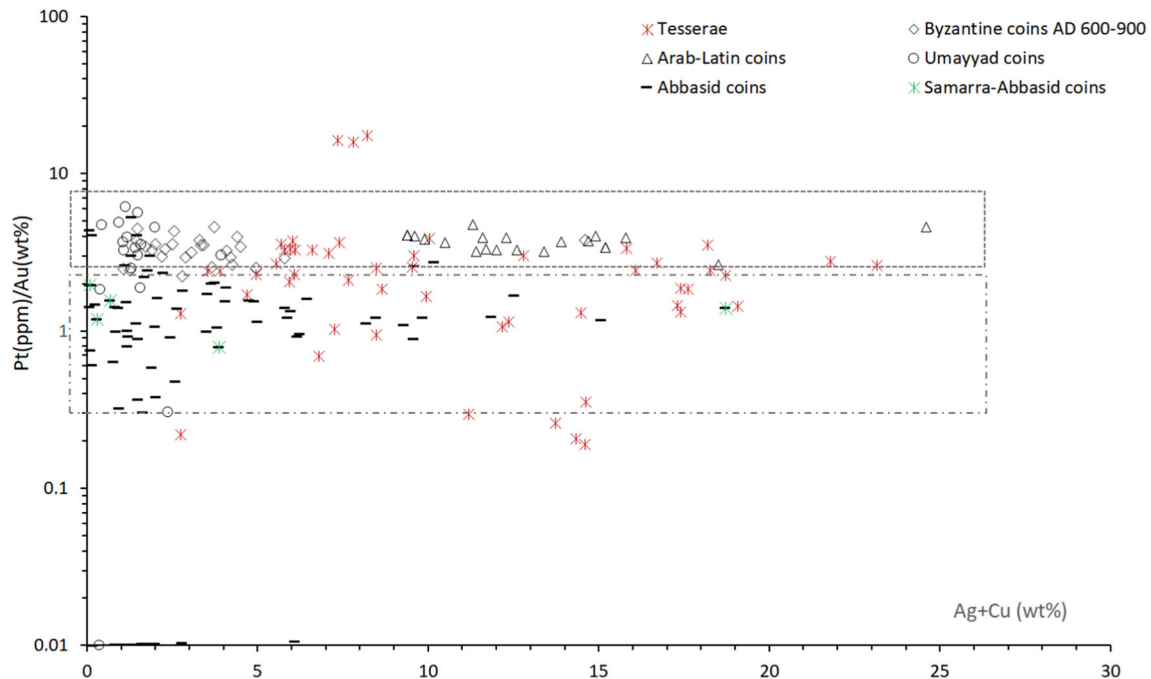

Fig. 7 Ratio Pt/Au versus Ag + Cu for the Islamic tesserae analysed in this work and published by Schibille [34], compared to data published for Byzantine [58] and Islamic coins [63, 64]

five Abbasid dinars struck in Samarra in Iraq [63], highlighted in Fig. 7, contain Pt amounts expected for the "Abbasid/local" gold. According to Leal [151], Samarra housed the most known ninth-century centre of mosaics production.

The results obtained do not support that gold, workers, and tesserae were given to the Umayyad caliph Al-Walīd by the Byzantine emperor for the Mosque of Damascus, as mentioned by al-Ya'qubi in the ninth century [152]. Al-Tabari (tenth century), who mentions the same, adds that the Byzantine emperor gave orders to search for mosaic cubes in ruined cities to be sent to al-Walīd

[153]. It is possible that he referred instead to al-Walid's decision to rebuild the Mosque of the Prophet at Medina [154], but it is also possible that the gold (or the gold leaf tesserae) given by the Byzantine Emperor only covered part of the huge quantity necessary.

4 Conclusion

Using the non-destructiveness of XRF methods, we have proposed in this work an analytical protocol to determine the major and trace element composition of gold leaf. Sequential analysis of the same area by using incident synchrotron radiation and three different experimental conditions provides the measurement of three groups of elements—those with characteristic lines below the Au–L-lines, those with characteristic lines higher than the Au–L-lines, and those with characteristic lines overlapping the Au–L-lines—with detection limits that range from 1 to 6 mg/kg. Although with slightly poorer detection limits than those that can be achieved by LA–ICP–MS, but sufficient to provenance gold, this non-destructive SRXRF protocol allows not only repeated analysis of the same areas of the gold leaf by using either the same technique or other techniques, but also the preservation of the samples for any further analytical study.

The detection limits of SRXRF can be improved by measuring a single element at optimised conditions instead of a group of elements. In the case of high-purity gold alloys, trace elements requiring measurement improvement are those with close adjacent fluorescence energies to the Au–L-lines. The most challenging situation is the analysis of Pt in very low concentrations. To test the validity of our protocol, we considered in this work the analysis of Pt in gold leaf < 0.5 µm thick. Gold leaf tesserae from fourth–ninth-century mosaics decorating nine Eastern and Western religious buildings were analysed by D^2XRF. During this period changes of gold supply are expected, from Roman to Byzantine gold and then to Islamic gold. In addition, Pt is one of the most characteristic elements of Roman gold and the only one so far measured for Byzantine gold. Although all the elements present in the gold alloys are measurable by SRXRF analysis, to increase the number of analysed samples and thus reduce the necessary beamtime, the major element concentrations were analysed by µXRF.

The results obtained have shown that the alloys used in the production of the gold leaf tesserae are identical to those commonly used in gilding. Gold leaf is produced by plastic deformation, which requires the use of high-purity gold alloys, with high ductility and malleability. Although monetary gold alloys are often of high-purity, the results do not support the hammering of gold coins to produce gold leaf during the considered period. By comparing the data obtained in this work with data published for tesserae collected in the same sites and others, we observed that all tesserae containing higher amounts of Cu and Ag were collected in Eastern sites. The majority of the gold leaf tesserae so far analysed made from the purest alloys were collected in Aachen, Maastricht, and Arles. Although the composition of the alloys does not indicate the origin of the gold, this result tends to support the existence of some local productions or specific supplies.

The increase of the amounts of Pt in the Roman gold after the currency reforms of 365–368 AD provides chronological criteria for the fourth-century tesserae, suggesting an earlier production for those from Noheda than for those from Arles, Jerusalem, and Milan. On the contrary, the gold leaf produced in the sixth century seems to be made from gold from different origins, containing amounts of Pt that only partially correspond to those contained in Byzantine coins minted until the ninth century. This can be a consequence of the use of gold alloys produced by mixing two or more types of gold, but we are unable to provide further discussion without further analytical results. Finally, we have shown that the gold leaf tesserae from the Mosque of Damascus were produced by using two sorts of gold, identical to the Byzantine/Umayyad and the Abbasid/local minted gold.

Data availability statement All data generated or analysed during this study are included in this article.

Declarations

Conflict of interest The authors have no financial or proprietary interests in any material discussed in this article.

References

1. L. James, *Mosaics in the Medieval World* (University Press, Cambridge, 2017)
2. M. Bartoli, F. Felici, P. Santopadre, M. Verità, in Bollettino icr 26, 211 (2015)
3. E.H. Swift, AJA. (1934). https://doi.org/10.2307/498933
4. C.L. Connor, *Saints and Spectacle* (Oxford University Press, 2016)
5. G. Bustacchini, Gold Bull. (1973). https://doi.org/10.1007/BF03215187
6. B. Schellewald, ZfK. (2016). https://doi.org/10.1515/ZKG-2016-0035
7. G. Hass, J. Opt. Soc. Am. (1955). https://doi.org/10.1364/JOSA.45.000945
8. R. Groth, W. Reichelt, Gold Bull. (1974). https://doi.org/10.1007/BF03215039
9. C. Bolgia, in *New light on old glass*. ed. by L. James, C. Entwistle (The British Museum Press, London, 2013), p.217

10. V. Ivanovici, in Colour and Light in Ancient and Medieval Art, ed. By C.N. Duckworth, A.E. Sassin (Routledge, London, 2017) p. 79
11. P. Mastoras, in *Glass, wax and metal*. ed. by I. Motsianos, K.S. Garnett (Archaeopress, Oxford, 2019), p.217
12. A.K.R. Choudhury, *Principles of colour appearance and measurement 1* (Woodhead Publishing, 2014)
13. W.J. Adams, J.H. Elder, PLoS Comput. Biol. (2014). https://doi.org/10.1371/journal.pcbi.1003576
14. T. Matsumoto, K. Fukuda, K. Uchikawa, Int. J. Affec. Eng. (2016). https://doi.org/10.5057/ijae.IJAE-D-16-00003
15. V. Honson, Q. Huynh-Thu, M. Arnison, D. Monaghan, Z.J. Isherwood, J. Kim, Front. Psychol. (2020). https://doi.org/10.3389/fpsyg.2020.00485
16. M. Verità, Quader. Friul. di Archeologia. **16**, 7 (2006)
17. M. Verità, P. Santopadre, J. Glass. Stud. **52**, 11 (2010)
18. M. Verità, Stud. Conserv. (2000). https://doi.org/10.1179/sic.2000.45.s3.007
19. M. Verità, in *Conservation of the Last Judgment Mosaic*. ed. by F. Piqué, D. Stulik (J. Paul Getty Trust, Los Angeles, 2004), p.123
20. A. Silvestri, S. Maltoni, C.L. Serra, J. Archaeol. Sci. Rep. (2022). https://doi.org/10.1016/j.jasrep.2022.103381
21. Q. Wu, M. Döbeli, T. Lombardo, K. Schmidt-Ott, B. Watts, F. Nolting, D. Ganz, Herit. Sci. (2020). https://doi.org/10.1186/s40494-020-00456-2
22. M.T. Wypyski, DOP. (2005). https://doi.org/10.2307/4128756
23. R. Arletti, C. Fiori, M. Vandini, Archaeometry (2010). https://doi.org/10.1111/j.1475-4754.2009.00504.x
24. A. Silvestri, S. Tonietto, G. Molin, J. Archaeol. Sci. (2011). https://doi.org/10.1016/j.jas.2011.07.027
25. L. James, G.J. Leigh, N. Schibille, Antiq. J. (2013). https://doi.org/10.1017/S0003581513000255
26. E. Neri, I. Biron, M. Verità, Archaeol. Anthropol. Sci. (2018). https://doi.org/10.1007/s12520-017-0492-7
27. L.W. Adlington, M. Ritter, N. Schibille, PLoS ONE (2020). https://doi.org/10.1371/journal.pone.023973210.1371/journal.pone.0239732
28. N. Schibille, C. Boschetti, M.Á. Valero Tévar, E. Veron, A.J. de Juan, Minerals. **10**(3), 272 (2020). https://doi.org/10.3390/min10030272
29. K. Dark, J. Kostenec, *Hagia Sophia in Context* (Oxbow Books, Oxford, 2019)
30. N.B. Teteriatnikov, *Mosaics of Hagia Sophia, Istanbul* (Dumbarton Oaks, Washington, D.C., 1998)
31. J. Sasaki, in Conservation and Presentation of Mosaics, ed. By J. M. Teutonico, L. Friedman, A. Ben Abed, R. Nardi (The Getty Conservation Institute, Los Angeles, 2017), p. 111.
32. A. Moropoulou, A. Bakolas, M. Karoglou, E.T. Delegou, K.C. Labropoulos, N.S. Katsiotis, J. Cult. Herit. (2013). https://doi.org/10.1016/j.culher.2013.01.006
33. A. Moropoulou, N. Zacharias, E.T. Delegou, B. Maróti, Z. Kasztovszky, Microchem. J. **125**, 170–184 (2016). https://doi.org/10.1016/j.microc.2015.11.020
34. N. Schibille, *Islamic Glass in the Making* (University Press, Leuven, 2022)
35. A. Stella, M. Verita, Mikrochim. Acta. (1994). https://doi.org/10.1007/BF01244574
36. P. Loukopoulou, A. Moropoulou, in *New light on old glass*. ed. by L. James, C. Entwistle (The British Museum Press, London, 2013), p.76
37. P. Loukopoulou, A. Moropoulou, in *Nondestructive Evaluation and Monitoring Technologies, Documentation, Diagnosis and Preservation of Cultural Heritage*. ed. by A. Osman, A. Moropoulou (Springer Cham, 2019), p.51
38. M. Hidaka, J. Miyata, Conservation of Monuments in the Mediterranean Basin, ed. By M. Koui, F. Zezza, D. Kouis (Springer Cham, 2018), p. 497
39. M. Verità, L. Lazzarini, E. Tesser, F. Antonelli, Archaeol. Anthropol. Sci. (2017). https://doi.org/10.1007/s12520-017-0559-5
40. A. Conventi, E. Neri M. Verità, *IOP Conf Ser Mater Sci Eng*. (2012) https://doi.org/10.1088/1757-899x/32/1/012007
41. E. Neri, M. Verità, J. Archaeol. Sci. (2013). https://doi.org/10.1016/j.jas.2013.07.017
42. B. Neuray, C. Fontaine, H. Wouters, in *Early Medieval Tesserae in Northwestern Europe*. ed. by L. Van Wersch, L. Verslype, D. Strivay, F. Theuws (Habelt-Verlag, Bonn, 2019), p.110
43. D. Moro, G. Ulian, G. Valdrè, Measurement (2018). https://doi.org/10.1016/j.measurement.2018.07.025
44. M.F. Guerra, NIM-B. (2004). https://doi.org/10.1016/j.nimb.2004.02.019
45. M.F. Guerra, X-ray Spectrom. (2008). https://doi.org/10.1002/xrs.1013
46. E. Neri, M. Verità, I. Biron, M.F. Guerra, J Archaeol Sci. (2016). https://doi.org/10.1016/j.jas.2016.05.003
47. M. Verità, L. Lazzarini, P. Santopadre, in *The Restoration of the Nativity Church in Bethlehem*. ed. by C. Alessandri (Taylor & Francis Group, London, 2020), p.189
48. Ph. Colomban, T. Calligaro, C. Vibert-Guigue, Q.L. Nguyen, H.G.M. Edwards, Archeo. Sci. (2005). https://doi.org/10.4000/archeosciences.424
49. M.A. Gómez-Morón, T. Palomar, L.C. Alves, P. Ortiz, M. Vilarigues, N. Schibille, J. Archaeol. Sci. **129**, 105370 (2021). https://doi.org/10.1016/j.jas.2021.105370
50. I. Tissot, N. Tissot, M. Manso, L.C. Alves, M.A. Barreiros, T. Marcelo, M.L. Carvalho, V. Corregidor, M.F. Guerra, NIM-B. (2013). https://doi.org/10.1016/j.nimb.2012.11.054
51. T. Panhuysen, A. Kronz, K. Simon, L. Van Wersch, in *Early Medieval Tesserae in Northwestern Europe*. ed. by L. Van Wersch, L. Verslype, D. Strivay, F. Theuws (Habelt-Verlag, Bonn, 2019), p.96
52. A. Kronz, K. Simons, W. Giertz, S. Ristow, in METALLA S7 66 (2015)
53. I. Coutinho, T. Medici, R.J.C. Silva, B. Gratuze, H. Catarino, A. Lima, J Archaeol. Sci. Rep. (2016). https://doi.org/10.1016/j.jasrep.2016.02.010
54. M. Blet-Lemarquand, S. Nieto-Pelletier, B. Gratuze, in *Metallurgy in Numismatics 6*. ed. by K.A. Sheedy, G. Davis (The Royal Numismatic Society, London, 2020), p.195
55. M.F. Guerra, Phys. Sci. Rev. (2018). https://doi.org/10.1515/psr-2018-0015
56. M.F. Guerra, Archaeometry (2021). https://doi.org/10.1111/arcm.12710
57. M.F. Guerra, T. Calligaro, J. Archaeol. Sci. (2004). https://doi.org/10.1016/j.jas.2002.05.001
58. A. Gondonneau, M.F. Guerra, J.N. Barrandon, Rev. d'Archéométrie. (1996). https://doi.org/10.3406/arsci.1996.934
59. M.F. Guerra, C.O. Sarthre, A. Gondonneau, J.-N. Barrandon, J. Archaeol. Sci. (1999). https://doi.org/10.1006/jasc.1999.0405
60. M.F. Guerra in Cultural Heritage Conservation and Environmental Impact Assessment by Non-Destructive Testing and Micro-Analysis, ed. By R. Van Griecken, K. Janssen (Balkema, London, 2005), p. 223
61. J. Poirier, Contribution à l'analyse de l'or antique. Application aux monnayages du monde méditerranéen du IIe au XIVe siècle (PhD, University of Orléans, 1983)
62. G.A. Green, D. Smythe, J. Archaeol. Sci. Rep. (2021). https://doi.org/10.1016/j.jasrep.2021.103128
63. A. Gondonneau, M.F. Guerra, Archaeometry (2002). https://doi.org/10.1111/1475-4754.t01-1-00087
64. T. Jonson, M. Blet-Lemarquand, C. Morrisson, Rev Numis. (2014) http://www.persee.fr/doc/numi_0484-8942_2014_num_6_171_3263
65. C. Morrisson, J.N. Barrandon, J. Poirier, in *L'or monnayée 2*. ed. by C. Morrisson, C. Brenot, J.N. Barrandon, J.P. Callu, J. Poirier, R. Halleux (CNRS, Paris, 1985), p.113
66. M.F. Guerra, T. Calligaro, M. Radtke, I. Reiche, H. Riesemeier, NIM-B. (2005). https://doi.org/10.1016/j.nimb.2005.06.150
67. M.F. Guerra, M. Radtke, I. Reiche, H. Riesemeier, E. Strub, NIM-B. (2008). https://doi.org/10.1016/j.nimb.2008.03.008

68. M. Radtke, I. Reiche, U. Reinholz, H. Riesemeier, M.F. Guerra, Anal. Chem. (2013). https://doi.org/10.1021/ac3025416
69. M.F. Guerra, I. Tissot, J. Archaeol. Sci. Rep. (2022). https://doi.org/10.1016/j.jasrep.2022.103477
70. R. Glaus, J. Koch, D. Günther, Anal. Chem. (2012). https://doi.org/10.1021/ac3008626
71. J. Flock, M. Haller, M. Haschke, *X-Ray Fluorescence Spectroscopy for Laboratory Applications* (Wiley-VCH, Weinheim, 2021)
72. M.B. Fricker, D. Kutscher, B. Aeschlimann, J. Frommer, R. Dietiker, J. Bettmer, D. Günther, Int. J. Mass Spectrom. (2011). https://doi.org/10.1016/j.ijms.2011.01.008
73. R. Kovacs, S. Schlosser, S. Staub, A. Schmiderer, E. Pernicka, D. Günther, J. Anal. At Spectrom. (2009). https://doi.org/10.1039/B819685K
74. M. Radtke, U. Reinholz, R. Gebhard, Archaeometry (2017). https://doi.org/10.1111/arcm.12294
75. I. Tissot, L.G. Troalen, M. Manso, M. Ponting, M. Radtke, U. Reinholz, M.A. Barreiros, I. Shaw, M.L. Carvalho, M.F. Guerra, Spectrochim. ACTA B At Spectrosc. (2015). https://doi.org/10.1016/j.sab.2015.03.012
76. M. Radtke, A.G. Buzanich, U. Reinholz, H. Riesemeier, O. Scharf, P. Scholz, M.F. Guerra, Microchem. J. (2016). https://doi.org/10.1016/j.microc.2015.10.039
77. O. Paris, C. Li, S. Siegel, G. Weseloh, F. Emmerling, H. Riesemeier, A. Erko, P. Fratzl, J. Appl. Cryst. (2007). https://doi.org/10.1107/S0021889806045444
78. E. Neri, M. Verità, in Il vetro in Italia, ed. By A. Coscarella (Ricerche 7, Università della Calabria, 2012), p. 13
79. E. Neri, V. Blanc Bijon 2016, in Estudios sobre mosaicos antiguos y medievales, ed. By L. Neira Jiménez (L'Erma di Bretschneider, Rome, 2016) p. 304
80. W. Giertz, S. Ristow, Antike Welt **5**, 59 (2013)
81. S. Ristow, in *Early Medieval Tesserae in Northwestern Europe*. ed. by L. Van Wersch, L. Verslype, D. Strivay, F. Theuws (Habelt-Verlag, Bonn, 2019), p.124
82. D. Robcis, C. Thomas, M. Aucouturier, in *Metal 2016*. ed. by R. Menon, C. Chemello, A. Pandya (ICOM-CC, New Delhi, 2013), p.235
83. A. Oddy, Gold Bull. (1981). https://doi.org/10.1007/BF03214601
84. C. Zievie, BIFAO. (1975) https://www.ifao.egnet.net/bifao/75/15/
85. M.F. Guerra, M. Martinón-Torres, S. Quirke, Ancient Egyptian gold (McDonald Institute Monographs, Cambridge, in press)
86. M.H. Crawford, J.M. Reynolds, ZPE. (1979) https://www.jstor.org/stable/20181398
87. M.J. Groen-Vallinga, L.E. Tacoma, in Work, Labour, and Professions in the Roman World, ed. By K. Verboven, C. Laes (Brill, Leiden, Boston, 2017) p. 104
88. C. Hawkins, *Roman artisans and the urban economy* (University Press, Cambridge, 2016)
89. I. Ferris, *The Dignity of Labour* (Amberley Publishing, Gloucestershire, 2021)
90. M. Berthelot, Ch. Ém, *Ruelle, Collection des anciens alchimistes grecs 3* (G. Steinheil, Paris, 1888)
91. H. Rackham, *Pliny Natural History* (Harvard Press and Heinemann, Cambridge, 1961)
92. G. Milanesi, C. Milanesi, *Il libro dell'arte o Trattato della Pittura, Cennino Cennini* (Le Monnier, Florence, 1859)
93. L. Belossi, A. Rossi, *Le vite de' piu eccellenti pittori, scultori, e architettori di Giorgio Vasari 1550* (Einaudi, Turin, 1986)
94. H. Burns, Mitt des Kunsthist. Inst. Florenz **23**, 145 (1979)
95. P. Grierson, in *Metallurgy in Numismatics 2*. ed. by W.A. Oddy, M.M. Archibald (The Royal Numismatic Society, London, 1988), p.95
96. A.M. Stahl, *Zecca* (Johns Hopkins Press, Baltimore, 2000)
97. C.M. Cipolla, *Money in Sixteenth-Century Florence* (University of California Press, Berkeley, 1989)
98. E.D. Nicholson, Gold Bull. (1979). https://doi.org/10.1007/BF03215119
99. M.G. Blaber, M.J. Ford, M.B. Cortie, in Gold, science and applications, ed. By C. Corti, R. Halliday (CRC Press, Taylor & Francis Group, 2010), p. 13
100. N.M. Ferreira-Alves, Revis. da Fac. de Letras. CTP **3**, 85 (2004)
101. P. Hatchfield, R. Newman, in *Gilded wood conservation and history*. ed. by D. Bigelow, E. Cornu, G.J. Landrey, C. Van Horne (Sound View Press, Madison, 1991), p.27
102. E. Darque-Ceretti, E. Felder, M. Aucouturier, Revista. Matéria. (2011). https://doi.org/10.1590/S1517-70762011000100002
103. A. Abdrabou, M. Abdallah, E. Nabil, Y. Matsuda, H.M. Kamal, Conservar Património. **30**, 9–19 (2019). https://doi.org/10.14568/cp2017033
104. C. Fourdrin, S.P. Camagna, C. Pacheco, M. Radepont, Q. Lemasson, B. Moignard, L. Pichon, B. Bourgeois, V. Jeammet, Microchem. J. **126**, 446–453 (2016)
105. A. Buccolieri, E. Degl'Innocenti, R. Cesareo, A. Castellano, G. Buccolieri, Measurement (2018). https://doi.org/10.1016/j.measurement.2018.05.063
106. D. Lesigyarski, B. Zlateva, V. Lyubomirova, T. Stoyanov, I. Kuleff, Archeo Sci. (2015). https://doi.org/10.4000/archeosciences.4440
107. P. Dandridge, in *Gilded metals*. ed. by T. Drayman-Weisser (Archetype, London, 2000), p.123
108. A.V. Zazhigalov, S.A. Balakin, I.V. Bacherikova, V.A. Zazhigalov, Chimie, physique et technologie des surfaces 1, 209 (2010)
109. J.V. García Marsilla, in *Sources sérielles et prix au Moyen-Âge*, ed. By C. Denjean (Toulouse, Presses du Midi, 2009), p. 253
110. M. Serrano y Sanz, in Revista de archivos, bibliotecas y museos 31, 433 (1914)
111. P. Meyers, Archaeometry (1969). https://doi.org/10.1111/j.1475-4754.1969.tb00630.x
112. J.P. Callu, C. Brenot, J.N. Barrandon, J. Poirier, in *L'or monnayée 2*. ed. by C. Morrisson, C. Brenot, J.N. Barrandon, J.P. Callu, J. Poirier, R. Halleux (CNRS, Paris, 1985), p.81
113. W.A. Oddy, V.E.G. Meyer, in *Excavations at Helgö X*. ed. by B.E. Hovén (Almqvist & Wiksell, Stockholm, 1986), p.153
114. W.E. Metcalf, W.J. Fulco, AJN 7/8, 145 (1995–1996)
115. W. Williams, J. Flanagan, MRS Proc. (1997). https://doi.org/10.1557/PROC-462-155
116. M. Hall, F. Kovacs, Bull. Metals Museum. **30**, 52 (1998)
117. M. Alram, M. Blet-Lemarquand, P.O.Skjærvø, in Des Indo-Grecs aux Sassanides, ed. By R. Gyselen (Res orientales XVII, 2007), p. 11
118. M.C. Vrij, The numismatic iconography of the period of Iconomachy (PhD thesis, University of Birmingham, 2016)
119. R. Naismith, Speculum (2014). https://doi.org/10.1017/S0038713413004533
120. M. McCormick, *Origins of the European Economy* (University Press, Cambridge, 2001)
121. C.S. Smith, J.G. Hawthorne, Trans. Am. Philos. (1974) https://www.jstor.org/stable/1006317
122. M.F. Hendy, ByzZ. (1972). https://doi.org/10.1515/byzs.1972.65.1.57
123. C. Morrisson, in The Economic History of Byzantium, ed. By A.E. Laiou (Dumbarton Oaks, Washington D.C., 2002), p. 909
124. J. Banaji, *Agrarian Change in Late Antiquity* (University Press, Oxford, 2001)
125. W. Davies, Early Med. Eur. **2**, 149–174 (2002). https://doi.org/10.1111/1468-0254.00106
126. G. Taylor, ASQ **32**, 6 (2010)
127. N. Oikonomidès, *Fiscalité et exemption fiscale à Byzance* (Institut de recherches byzantines, Athens, 1996)
128. AHM Jones, *The Later Roman Empire* (Blackwell, Oxford, 1964)

129. J.E. Healy, *Mining and Metallurgy in the Greek and Roman World* (Thames and Hudson, London, 1978)
130. A.M. Hirt, *Imperial Mines and Quarries in the Roman World* (University Press, Oxford, 2010)
131. A. Orejas, F.J. Sánchez-Palencia, AJA. (2002). https://doi.org/10.2307/4126218
132. B. Pitarakis, Rev Numis. (1998) https://www.persee.fr/doc/numi_0484-8942_1998_num_6_153_2196
133. C. Meyer, JOM. (1997). https://doi.org/10.1007/BF02914661
134. S. Vryonis, Speculum (1962). https://doi.org/10.2307/2850595
135. K.P. Matschke, in The Economic History of Byzantium, ed. A.E. Laiou (Dumbarton Oaks, Washington D.C, 2002), p. 115
136. J.C. Edmondson, JRS. (1989). https://doi.org/10.2307/301182
137. C. Pharr, *The Theodosian Code and Novels* (Princeton University Press, New Jersey, 1952)
138. B.W. Frier, *The Codex of Justinian* (University Press, Cambridge, 2016)
139. S. Moorhead, Handb. Greek Roman Coin. (2012). https://doi.org/10.1093/oxfordhb/9780195305746.013.0033
140. K. Painter, Ant J. (1972). https://doi.org/10.1017/S0003581500020151
141. M.F. Hendy, Studies in the Byzantine Monetary Economy C. 300–1450 (University Press, Cambridge, 1985)
142. P. Grierson, M. Blackburn, *Medieval European Coinage 1* (University Press, Cambridge, 1986)
143. F. Baratte, Lingots d'or et d'argent en rapport avec l'atelier de Sirmium Sirmium **8**, 101 (1978)
144. L. Treadwell, Rev Numis. (2009) https://www.persee.fr/doc/numi_0484-8942_2009_num_6_165_2879
145. M.L. Bates, in *North Africa from Antiquity to Islam*. ed. by M. Horton, T. Wiedemann (University Press, Bristol, 1995), p.12
146. C. Foss, in *Money, Power and Politics in Early Islamic Syria*. ed. by J. Haldon (Burlington, Ashgate, 2010), p.75
147. S. O'Sullivan, Doc. Hist. Early Islam. World. (2015). https://doi.org/10.1163/9789004284340_006
148. G.W. Heck, in *Money, Power and Politics in Early Islamic Syria*. ed. by J. Haldon (Ashgate, Burlington, 2010), p.97
149. G. H. Qaddumi, A Medieval Islamic Book of Gifts and Treasures (PhD thesis, Harvard University, 1990)
150. S. Heidemann, Iran (1998). https://doi.org/10.2307/4299978
151. B. Leal, Muqarnas (2020). https://doi.org/10.1163/22118993-00371P03
152. M.S. Gordon, C.F. Robinson, E.K. Rowson, M. Fishbein, *The Works of Ibn Wāḍiḥ al-Yaʿqūbī 3* (Leiden, Boston, Brill, 2018)
153. H.A.R. Gibb, DOP **12**, 219 (1958)
154. A. Cutler, DOP. (2001). https://doi.org/10.2307/1291821